

PCCP

Accepted Manuscript



This is an *Accepted Manuscript*, which has been through the Royal Society of Chemistry peer review process and has been accepted for publication.

Accepted Manuscripts are published online shortly after acceptance, before technical editing, formatting and proof reading. Using this free service, authors can make their results available to the community, in citable form, before we publish the edited article. We will replace this *Accepted Manuscript* with the edited and formatted *Advance Article* as soon as it is available.

You can find more information about *Accepted Manuscripts* in the [Information for Authors](#).

Please note that technical editing may introduce minor changes to the text and/or graphics, which may alter content. The journal's standard [Terms & Conditions](#) and the [Ethical guidelines](#) still apply. In no event shall the Royal Society of Chemistry be held responsible for any errors or omissions in this *Accepted Manuscript* or any consequences arising from the use of any information it contains.

**Halogen-bond and Hydrogen-bond Interactions between Three Benzene
Derivatives and Dimethyl Sulphoxide**

Yan-Zhen Zheng,^a Nan-Nan Wang,^{a,b} Yu Zhou^a and Zhi-Wu Yu^{a*}

^a*Key Laboratory of Bioorganic Phosphorous Chemistry and Chemical Biology
(Ministry of Education), Department of Chemistry, Tsinghua University, Beijing
100084, P. R. China*

^b*State Key Laboratory of Science and Technology on Advanced Ceramic Fibers and
Composites, College of Aerospace Science and Engineering, National University of
Defence Technology, Changsha, Hunan 410073, China.*

***To whom correspondence should be addressed.**

Dr. Zhi-Wu Yu

Tel. (+86) 10 6279 2492

Fax. (+86) 10 6277 1149

Email: yuzhw@tsinghua.edu.cn

Abstract

Halogen-bond, like hydrogen-bond, is a kind of noncovalent interaction and plays important roles in diverse fields including chemistry, biology and crystal engineering. In this work, a comparative study was carried out to examine the halogen/hydrogen-bonding interactions between three fluoro-benzene derivatives and dimethyl sulphoxide (DMSO). A number of conclusions were obtained by using attenuated total reflection infrared spectroscopy (ATR-IR), nuclear magnetic resonance (NMR) and ab initio calculations. Electrostatic surface potential, geometry, energy, vibrational frequency, intensity and the natural population analysis (NPA) charge of monomers and complexes are studied at the MP2 level of theory with the aug-cc-pVDZ basis set. First, the interaction strength decreases in the order $C_6F_5H-DMSO > ClC_6F_4H-DMSO > C_6F_5Cl-DMSO$, implying that the hydrogen-bond is stronger than the halogen-bond in the systems and, when interacting with ClC_6F_4H , DMSO favors to form hydrogen-bond rather than halogen-bond. Second, attractive energy dependences on $1/r^{3.3}$ and $1/r^{3.1}$ were established for the hydrogen-bond and halogen-bond, respectively. Third, upon the formation of hydrogen-bond and halogen-bond, charge transfers from DMSO to the hydrogen-bond and halogen-bond donor. Back group CH_3 was found to contribute positively to stabilize the complexes. Fourth, an isobestic point was detected in the $\nu(C-Cl)$ absorption band in $C_6F_5Cl-DMSO-d_6$ system, indicating that there are only two dominating existing forms of C_6F_5Cl in the binary mixtures, non-complexed and halogen-bond complexed forms. The presence of stable complexes in $C_6F_5H-DMSO$ and $ClC_6F_4H-DMSO$ systems are evidenced by the appearance of new peaks with fixed positions.

1. Introduction

Noncovalent interactions have attracted increasing interest in chemistry, biology and many interdisciplinary sciences.¹⁻⁹ Among various types of noncovalent interactions, without doubt, hydrogen-bond is the most important and has been studied extensively in both theoretical and experimental aspects.¹⁻⁴ In recent years, a specific noncovalent interaction involving halogen atoms as electron acceptors has also been found to play important roles similar to the case of hydrogen-bond.¹⁰ This is called halogen-bond. The first report of halogen-bond was from Guthrie in 1863.¹¹ It is now recognized as the interaction of a halogen atom X in the molecule RX with a negative charge site of a neighboring molecule. Here X can be fluorine, chlorine, bromine or iodine, and R is an electronegative substituent.^{12,13} Halogen-bond is an electrostatically-driven interaction, owing to the existence of a region of positive electrostatic potential on the outermost surface of X, centered on the extension of the covalent bond R-X.¹⁴⁻¹⁷ The positive region, called a “ σ -hole”, is dependent on the polarizability of the halogen, which increases with the increasing size and decreasing electronegativity of the halogen X ($\text{Cl} < \text{Br} < \text{I}$),¹⁵ and the electron withdrawing ability of R.¹⁸ In the σ -hole model, of peculiar interest is that a halogen atom exhibits both electrophilicity along the C-X axis and nucleophilicity perpendicular to the axis.¹⁵ In other words, the halogen atom can act both as an electron acceptor in the positively charged region of σ -hole or an electron donor in the ring region around the C-X axis.

Efforts have been made to compare the properties of halogen-bonds and

hydrogen-bonds. It was found that they are quite similar: (1) Both halogen-bonds and hydrogen-bonds have directivity and selectivity.¹⁹ (2) They present conventional red-shift and unconventional blue-shift halogen-bonds and hydrogen-bonds.^{20,21} (3) Formation of halogen/halogen-bond complexes is closely related to electrostatic effect, polarization and dispersion.^{22,23} Thus, some existing explanations for hydrogen-bonds can also be used to explain halogen-bonds. Nevertheless, the electronic structures of the halogen atoms are quite different from that of the hydrogen atom. There must be some differences in the properties of the two types of bonds.

Most studies on halogen-bond have been on solid and gaseous systems. The former concerns with crystallography and related studies,⁵⁻⁹ whilst the latter includes quantum chemical calculations.^{12,16} Reports on liquid systems are relatively scarce. Examples include the thermodynamic investigations of haloarenes^{24,25} and haloalkanes²⁴. To enrich our knowledge on the halogen bonding interactions in liquids, we carried out a comparative study on halogen-bond and hydrogen-bond interactions of liquid systems in this work. Three fluoro-benzene derivatives were chosen as halogen/hydrogen donors. They are 1,2,3,4,5-pentafluorobenzene (C_6F_5H), 1-chloro-2,3,4,5,6-pentafluorobenzene (C_6F_5Cl), and 1-chloro-2,3,5,6-tetrafluorobenzene (ClC_6F_4H). Dimethyl sulphoxide (DMSO) was selected as the acceptor because it is an aprotic super solvent.²⁶ Clark et.al have dealt with dimethyl sulfoxide and halogen/hydrogen-bonding in theory aspect.²⁷

Among various experimental techniques, IR is a convenient and effective approach to study hydrogen-bonding and halogen-bonding interactions at the molecular

level.^{28,29} We have thus investigated the hydrogen/halogen-bonding properties of the three binary systems using ATR-FTIR, NMR (¹H NMR and ¹⁹F NMR) and ab initio calculation. In order to get rid of overlap in the C–H stretching vibration region of C₆F₅H/C₆F₄ClH and DMSO, deuterated dimethyl sulphoxide (DMSO-*d*₆) was used in the FTIR study. In particular, excess infrared spectroscopy^{30–39} and two-dimensional correlation spectroscopy (2D-COS)^{40,41} have been employed to reveal details of the molecular interactions.

2. Results and Discussion

2.1. Electrostatic Surface Potentials of Single Molecules

Figure 1 displays electrostatic surface potentials (ESP) of C₆F₅H, C₆F₅Cl, ClC₆F₄H and DMSO. As would be anticipated, positive potential encompassing the hydrogen atoms and strong negative potential around the oxygen atom in DMSO are seen. In the three benzene derivatives, strong positive potentials encompass the hydrogen atoms and the aromatic rings, and negative potentials encompass the fluorine atoms. What is particularly interesting is that there is also a positive region on the outermost portion of each chlorine atom in C₆F₅Cl and ClC₆F₄H, centered on the intersection of its surface with the C–Cl axis. This makes it possible for the chlorine atoms in C₆F₅Cl and ClC₆F₄H to be electron acceptors.

2.2. ATR and Excess Infrared Spectra Analysis

The partial IR spectra of pure DMSO-*d*₆, DMSO and the three benzene derivatives are presented in Figure 2. The peaks around 3099 cm⁻¹ and 3092 cm⁻¹ are attributed to the ν(C–H) of pure C₆F₅H and ClC₆F₄H, and that at 880 cm⁻¹ and 911 cm⁻¹ are

attributed to the $\nu(\text{C-Cl})$ in $\text{C}_6\text{F}_5\text{Cl}$ and $\text{ClC}_6\text{F}_4\text{H}$, respectively.⁴² For pure $\text{DMSO-}d_6$ and DMSO , the bands over the 1000 cm^{-1} to 1100 cm^{-1} range are from $\nu(\text{S=O})$, two bands around 2125 and 2250 cm^{-1} are attributed to the $\nu_s(\text{C-D})$ and $\nu_{as}(\text{C-D})$ of $\text{DMSO-}d_6$, two bands around 2912 and 2995 cm^{-1} are attributed to the $\nu_s(\text{C-H})$ and $\nu_{as}(\text{C-H})$ of DMSO , respectively.⁴³

2.2.1. Sequential Order of the Interactions of C–H and C–Cl in $\text{ClC}_6\text{F}_4\text{H}$ with DMSO

As can be seen from the ESP map, both the hydrogen atom and the chlorine atom in $\text{ClC}_6\text{F}_4\text{H}$ can be electron acceptor in interacting with the oxygen atom in $\text{DMSO-}d_6$. To find out which one is the more favorite, $\nu(\text{C-H})$ and $\nu(\text{C-Cl})$ of $\text{ClC}_6\text{F}_4\text{H}$ are selected to do the two-dimensional correlation (2D-COS) analysis and the results are shown in Figure 3. As displayed in the figure, negative cross peaks at around $(3000\text{ cm}^{-1}, 911\text{ cm}^{-1})$ are seen in both the synchronous spectrum and asynchronous spectrum. According to Noda's rule,^{40,41} the change of the absorption band of the $\nu(\text{C-H})$ is prior to that of $\nu(\text{C-Cl})$. It means that the oxygen atom in DMSO prefers interacting with the hydrogen atom to the chlorine atom in $\text{ClC}_6\text{F}_4\text{H}$ when the amount of DMSO is not enough. This conclusion has been confirmed by quantum chemical calculation shown in Section 2.3.1. In the following analysis, for $\text{ClC}_6\text{F}_4\text{H-DMSO}$ system, we will focus on the $\nu(\text{C-H})$, rather than the $\nu(\text{C-Cl})$.

2.2.2. C–Cl stretching vibration in $\text{C}_6\text{F}_5\text{Cl}$

The IR and excess spectra in the $\nu(\text{C-Cl})$ region of the $\text{C}_6\text{F}_5\text{Cl-DMSO-}d_6$ systems are shown in Figure 4. In the ATR-FTIR spectra (Figure 4A), the only evident change

of the peak in the mixing process is the decreases in absorbance. The peak position of $\nu(\text{C}-\text{Cl})$ is red-shifted by only 0.5 cm^{-1} . The excess spectra, however, generate both positive and negative peaks and the positions of them are nearly fixed, indicating the possible appearing and disappearing forms of the concerned species. Most interestingly, when the original IR spectra are normalized by the corresponding concentration of $\text{C}_6\text{F}_5\text{Cl}$ and the light path length, there appears an isobestic point at 882.5 cm^{-1} as displayed in Figure 4C. This strongly suggests that $\text{C}_6\text{F}_5\text{Cl}$ exists in two distinct states upon dilution with DMSO, most likely halogen-bonded (as demonstrated in Figure 7B) and non-bonded forms. In an excess spectrum, the positive and negative peaks for a particular vibrational mode represent the increasing and decreasing amounts of the respective species including the interacting complexes in the mixture. The frequency of the $\nu(\text{C}-\text{Cl})$ in halogen bonded $\text{C}_6\text{F}_5\text{Cl}$ is lower than non-bonded $\text{C}_6\text{F}_5\text{Cl}$ according to the quantum calculations. This indicates that the non-bonded $\text{C}_6\text{F}_5\text{Cl}$ decreases and halogen-bonded increases in the mixture compared to pure $\text{C}_6\text{F}_5\text{Cl}$. Besides, as can be seen in Figure 4C, the gradually increasing and decreasing of the intensities in the lower and higher wavenumber of the isobestic point indicate that the non-bonded $\text{C}_6\text{F}_5\text{Cl}$ decreases and the halogen-bonded $\text{C}_6\text{F}_5\text{Cl}$ increases with increasing DMSO.

2.2.3. C–H stretching vibration in $\text{C}_6\text{F}_5\text{H}$ and $\text{ClC}_6\text{F}_4\text{H}$

Shown in Figure 5 are the IR and excess spectra in the aromatic C–H stretching vibration region. For pure $\text{C}_6\text{F}_5\text{H}$ and $\text{ClC}_6\text{F}_4\text{H}$, the peaks at 3099 cm^{-1} and 3092 cm^{-1} are attributed to the $\nu(\text{C}-\text{H})$ in the aromatic ring. With gradual addition of $\text{DMSO}-d_6$,

the absorbance of the band at 3099 cm^{-1} (Figure 5A) decreases gradually and a new broad band appears at lower wave number (3019 cm^{-1}). The new band has a greater integrated intensity than the band at 3099 cm^{-1} (normalized to unit concentration and path length), and it shows a continuous red-shift throughout. The results indicate that $\text{C}_6\text{F}_5\text{H}$ forms a hydrogen-bonded complex with DMSO.⁴⁴ The new peak is attributed to the $\nu(\text{C-H})$ in the hydrogen-bonded complex. In the $\text{ClC}_6\text{F}_4\text{H-DMSO}$ system, however, there appear two new broad peaks in the lower wavenumber region (Figure 5B). The two new peaks are attributed to the Fermi resonance between the aromatic C-H stretching vibration in the hydrogen-bonded complex and the doubling frequency of the aromatic ring vibration around 1500 cm^{-1} . The excess spectra present clearer evidence for the interactions. There are negative bands around 3099 and 3092 cm^{-1} in Figure 5C and 5D, indicating that the $\text{C}_6\text{F}_5\text{H}$ and $\text{ClC}_6\text{F}_4\text{H}$ monomers in the mixtures gradually decrease with increasing $\text{DMSO-}d_6$ concentration. The broad positive bands at lower wavenumber evidence the presence of $\text{C}_6\text{F}_5\text{H-DMSO}$ and $\text{ClC}_6\text{F}_4\text{H-DMSO}$ hydrogen-bonded complexes as present in quantum chemical section (Figure 7A and 7C).

The hydrogen-bonds of aromatic C-H have been classified in literatures as “proper red-shifted hydrogen-bonds”,³⁵⁻³⁸ characterized by a red-shift of the corresponding stretching vibration band and an increase of IR intensity. The appearance of the broad positive bands at lower wavenumber is in agreement with the participation of the aromatic C-H in $\text{C}_6\text{F}_5\text{H}$ and $\text{ClC}_6\text{F}_4\text{H}$ in forming hydrogen-bonds with DMSO, and that the hydrogen-bonds were strengthened in the mixture compared to the pure state.

2.2.4. C–D symmetrical stretching vibration in DMSO- d_6 methyl groups

In order to avoid the influence of overlap, $\nu_s(\text{C-D})$ of DMSO- d_6 was used to analyze the environmental change of DMSO upon dilution. Shown in Figure 6 are the partial ATR-FTIR of $\nu_s(\text{C-D})$ and the respective excess IR spectra of $\text{C}_6\text{F}_5\text{H-DMSO-}d_6$, $\text{ClC}_6\text{F}_4\text{H-DMSO-}d_6$ and $\text{C}_6\text{F}_5\text{Cl-DMSO-}d_6$ systems over the entire concentration range. Two obvious features can be seen readily in the original IR spectra (Figure 6A, B, C): the absorbance of $\nu_s(\text{C-D})$ decreases monotonically and the peaks gradually shift to higher wavenumber with increasing fluoro-benzene derivatives. It's known that both direct and indirect interactions may lead to the blue-shift and the decrease in absorptivity of $\nu_s(\text{C-D})$ in DMSO- d_6 . As will be demonstrated in the quantum chemical section, this is a result of the indirect effect arising from the interaction between S=O and the three benzene derivatives. Excess infrared spectra can better reveal the changes of the IR spectra than the original IR spectra as shown in Figure 6D–6F. A general feature of these excess spectra is the positive peaks at higher wavenumbers and negative peaks at lower wavenumbers. With decreasing mole fraction of DMSO- d_6 , the areas of the negative peaks increase and that of the positive band decrease gradually. Undoubtedly, the negative and positive peaks are from DMSO- d_6 molecules before and after dilution with the fluoro-benzene derivatives. The interesting point is that the positions of the positive and negative peaks are nearly fixed. This means that the DMSO molecules are not totally dispersed in the benzene derivatives. They may form interaction complex in the solution. For instance, the excess spectra of the $\text{C}_6\text{F}_5\text{Cl-DMSO-}d_6$ mixtures

produced positive and negative peaks located at about 2131 cm^{-1} and 2122 cm^{-1} , respectively. They are attributed to the absorption of the DMSO- d_6 complex with $\text{C}_6\text{F}_5\text{Cl}$ and that of DMSO- d_6 self-associates.

Another feature can be seen in Figure 6D, 6E, 6F is that the appearance of the negative bands in the excess spectra are different for the three systems. At the mole fraction (x_{DMSO}) of about 0.9, the negative band in the excess spectra of $\text{C}_6\text{F}_5\text{Cl}$ -DMSO- d_6 system is hardly seen, whilst that of $\text{C}_6\text{F}_5\text{H}$ -DMSO- d_6 and $\text{ClC}_6\text{F}_4\text{H}$ -DMSO- d_6 systems are pronounced. This indicates that $\text{C}_6\text{F}_5\text{H}$ and $\text{ClC}_6\text{F}_4\text{H}$ are the more powerful benzene derivative to break the self-associates of DMSO, thus giving a possible sequential order of the interaction strength of the three systems: $\text{C}_6\text{F}_5\text{H}$ -DMSO \sim $\text{ClC}_6\text{F}_4\text{H}$ -DMSO $>$ $\text{C}_6\text{F}_5\text{Cl}$ -DMSO. This conclusion is supported by the quantum chemical calculation as will be demonstrated in Section 2.3.1.

2.3. Quantum Chemical Calculations

2.3.1. Structures

The optimized geometries of individual molecules DMSO, $\text{C}_6\text{F}_5\text{H}$, $\text{C}_6\text{F}_5\text{Cl}$ and $\text{ClC}_6\text{F}_4\text{H}$, and the complexes of $\text{C}_6\text{F}_5\text{H}$ -DMSO, $\text{C}_6\text{F}_5\text{Cl}$ -DMSO and $\text{ClC}_6\text{F}_4\text{H}$ -DMSO were studied at the MP2/aug-cc-pVDZ level. The sum of van der Waals atomic radii of hydrogen and oxygen (2.5 \AA) and that of chlorine and oxygen (3.2 \AA) are used as critical values for judging the presence of hydrogen-bond and halogen-bond.⁴⁵

Figure 7 displays the optimized geometries of the three complexes. The corresponding interaction energies of the complexes are displayed below the structures. As can be seen in the figure, $\text{C}_6\text{F}_5\text{H}$ and $\text{C}_6\text{F}_5\text{Cl}$ interact with the oxygen

atom of DMSO forming hydrogen-bond and halogen-bond, and both of the hydrogen and the chlorine atoms in $\text{ClC}_6\text{F}_4\text{H}$ can interact with the oxygen atom in DMSO, forming hydrogen-bond and halogen-bond. The interaction energy of complex C is 15.8 kJ/mol lower than that of complex D, indicating that the former is much more stable than the latter. As a result, it is more likely for DMSO to interact with the hydrogen atom rather than the halogen atom in $\text{ClC}_6\text{F}_4\text{H}$ when the amount of DMSO is not enough. This is consistent with the 2D-COS results discussed in Section 2.2.1. In the following analysis, only the more stable $\text{ClC}_6\text{F}_4\text{H}$ -DMSO complex is considered. Based on the interaction energies shown in the figure, we can easily get the sequential order of the interaction strength: $\text{C}_6\text{F}_5\text{H}$ -DMSO \sim $\text{ClC}_6\text{F}_4\text{H}$ -DMSO $>$ $\text{C}_6\text{F}_5\text{Cl}$ -DMSO.

As shown in Figure 7, the optimized C-Cl \cdots O angles are 179° and 176°, very close to 180°, demonstrating the characteristic directionality of halogen-bonds. The small deviations could be attributed to secondary interactions involving $\text{C}_6\text{F}_5\text{Cl}/\text{ClC}_6\text{F}_4\text{H}$ and DMSO. In comparison, the optimized C-H \cdots O angles are much less than 180°, with deviations more than 13°, indicating that hydrogen-bonds are less directional than halogen-bonds.⁴⁶ This can be explained by the fact that the positive electrostatic potential of a concerned chlorine atom is on the outermost portion of the atom, centered around the intersection of its surface with the C-Cl axis (σ -hole), while the positive electrostatic potential of a hydrogen atom covers much larger area of the atomic surface (see Figure 1).

Table 1 and Table 2 list the selected geometrical and vibrational parameters of the

investigated complexes. As can be seen in Table 1, the C–H bonds in both C₆F₅H and ClC₆F₄H are elongated upon complexation. As can be seen in Tables 1 and 2, the elongations of the C–H bonds in C₆F₅H and ClC₆F₄H are concomitant with marked (greater than 89 cm⁻¹) decrease in the C–H stretching frequencies (red-shift) and big (greater than 310 km mol⁻¹) increase in the infrared intensities. These are in agreement with experimental results discussed in previous sections. Similar to C–H bonds, the C–Cl bonds also subject to changes upon halogen-bond formation. The data in Table 1 show that both of the C–Cl bonds in C₆F₅Cl and ClC₆F₄H are elongated upon complexation. And the elongations are concomitant with decreases in the C–Cl stretching frequencies (red-shift) and increase in the infrared intensity of the corresponding vibration modes. This is in agreement with the infrared results.

2.3.2. NBO analysis

Formation of hydrogen-bonds or halogen-bonds, either conventional or blue-shifted ones, accompanies with electron density rearrangement. Herein, charge distributions of the most stable hydrogen/halogen-bonded complexes were examined by means of the NBO analysis at the MP2/aug-cc-pVDZ level. Listed in Table 3 are some of the results.

As can be seen in the table, both hydrogen-bonding and halogen-bonding donor molecules gain charges upon complexation, with markedly larger gains for hydrogen-bond donors in C₆F₅H–DMSO and ClC₆F₄H–DMSO systems. This is because that the interactions in the two complexes are stronger than that in C₆F₅Cl–DMSO complex. As the halogen-bond donor, chlorine shows a decrease in

electron density in the C_6F_5Cl -DMSO complex, similar to a hydrogen atom when it works as the hydrogen-bond donor. The oxygen atoms in the three complexes all gain charges upon complexation. In addition, the methyl groups of DMSO in all the three complexes lose negative charges upon complexation. This is consistent with our previous findings in systems such as methanol-DMSO³⁰ and 1-butylpyridinium tetrafluoroborate-DMSO,³⁶ in which the methyl groups are back groups of the hydrogen-bond acceptors. In the case of hydrogen-bond donor, the chlorine atom in ClC_6F_4H -DMSO gains electron density, similar to the methyl group of methanol in the DMSO-methanol complex. Altogether, there is a charge transfer from hydrogen/halogen-acceptors (DMSO) to hydrogen/halogen-donors (C_6F_5H , ClC_6F_4H and C_6F_5Cl). The charge variations of the back groups take place to stabilize the complexes.

2.3.3. Energy Analysis

The energy of a hydrogen-bond or halogen-bond depends on the separation between the donor atom and acceptor atom. A comparative study was carried out by evaluating the distance dependences of the energies of C_6F_5Cl -DMSO and C_6F_5H -DMSO. Single point energies of the two complexes in their most stable forms as functions of the $C_6F_5-Cl\cdots O$ and $C_6F_5-H\cdots O$ separations were calculated and the results are shown in Figure 8. As can be seen in Figure 8A, with increasing separation, the energies change from positive to negative, indicating that the interactive nature changes from repulsive to attractive. There exist a position with lowest energy in each case, corresponding to the most stable optimized geometry shown in Figure 7A and

Figure 7B. The data can be fitted to a function of Lennard-Jones form $E=a/r^m-b/r^n$. For the halogen-bond, $m=8.5$ and $n=3.1$, whilst for the hydrogen-bond, $m=8.5$ and $n=3.3$. For the energies at the distance longer than the most stable optimized geometries, they can be fitted to a function containing only the attractive term $E=-b/r^n$. For the halogen-bond, $n=3.0$, whilst for the hydrogen-bond, $n=3.1$. Thus, the attractive energy of the halogen-bond decays a bit slower than that of the hydrogen-bond. It should be noted that our result on hydrogen-bond is very close to a recent publication by Wendler et al.⁴⁷ who reported a value of $m=3.8$.

2.4. NMR Analysis

^1H NMR and ^{19}F NMR measurements of pure $\text{C}_6\text{F}_5\text{H}$, $\text{ClC}_6\text{F}_4\text{H}$, $\text{C}_6\text{F}_5\text{Cl}$ and DMSO, and a series of $\text{C}_6\text{F}_5\text{H}$ -DMSO, $\text{ClC}_6\text{F}_4\text{H}$ -DMSO and $\text{C}_6\text{F}_5\text{Cl}$ -DMSO mixtures were carried out at 298 K, and the changes on chemical shift of individual hydrogen and fluorine atoms during the dilution process were evaluated. The chemical shift variations ($\Delta\delta$) are expressed by the differences between the chemical shifts of the mixtures and those of the pure chemicals.

2.4.1. ^1H NMR Analysis

Assignments of the ^1H NMR signals to the hydrogen atoms in $\text{C}_6\text{F}_5\text{H}$, $\text{ClC}_6\text{F}_4\text{H}$ and DMSO are displayed in Figure 9A. The dependences of $\Delta\delta$ of different hydrogen atoms on the mole fraction of DMSO are displayed in Figure 9B and 9C for the three binary mixtures. As can be seen in the figures, the $\Delta\delta$ values of the hydrogen atoms in $\text{C}_6\text{F}_5\text{H}$ and $\text{ClC}_6\text{F}_4\text{H}$ are all positive (Figure 9B), while those in DMSO are negative (Figure 9C). This states that the hydrogen atoms in the benzene derivatives gradually

move downfield with increasing concentration of DMSO, while the hydrogen atoms in DMSO move upfield with increasing benzene derivatives.

Hydrogen-bonding and anisotropy effect are two important factors that influence the chemical shift in C_6F_5H -DMSO, ClC_6F_4H -DMSO and C_6F_5Cl -DMSO systems. It is known that formation of hydrogen-bonds causes downfield chemical shift of the hydrogen atoms. The observation of the downfield changes on chemical shifts of hydrogen atoms in C_6F_5H and ClC_6F_4H is consistent with the conclusion drawn from FTIR and quantum calculation. In the case of DMSO, the observation of upfield shift of the hydrogen atoms could be explained as a result of the location of the hydrogen atoms in the shielding cone of the aromatic rings.

2.4.2. ^{19}F NMR Analysis

^{19}F NMR is another sensitive indicator to provide intermolecular interaction information involving fluorine-substituted molecules, thanks to its large chemical shift range and high intrinsic sensitivity (85% of 1H NMR). Assignments of the ^{19}F NMR signals to the fluorine atoms in C_6F_5H , C_6F_5Cl and ClC_6F_4H are displayed in Figure 10A. For the binary mixtures, the dependences of $\Delta\delta$ of the three benzene derivatives on the mole fraction of DMSO are displayed in Figure 10B–10D. As can be seen in the figures, all the $\Delta\delta$ values become more and more negative with increasing concentration of DMSO, meaning that the fluorine atoms gradually move upfield in the dilution process. This can be explained by the formation of halogen/hydrogen-bonding complexes as it is known that, upon forming halogen/hydrogen-bonds, electron transfers from acceptors to donors, causing upfield

move of the chemical shifts of the back groups.^{48,49} Detailed electron gains of the fluorine atoms in the three benzene derivatives upon forming hydrogen/halogen bond with DMSO have been calculated by quantum chemical method, and the results are summarized in Table 4. The results are in good agreement with the observed chemical shift changes of each fluorine atoms. Particularly, in the case of ClC₆F₄H, there are two possible bonding forms. When H plays the role of donor, the electron gains of F1 and F2 atoms are -0.0155 e and -0.0084 e, respectively, consistent with the fact that the chemical shift of F1 changes more pronounced than that of F2. On the contrary, when Cl is the donor, the electron gain of F1 is less than that of F2, against the ¹⁹F NMR results. Thus we conclude that DMSO prefers to interact with the hydrogen rather than the chlorine atom in ClC₆F₄H. It should be noted that the discussion is valid at low DMSO concentration when it interacts either with the H-end or Cl-end of ClC₆F₄H. At high concentration of DMSO, both positions of ClC₆F₄H could form hydrogen/halogen bond with DMSO. In this case, the electron density of F1 is also higher than that of F2 (Table 4), consistent with the NMR results.

3. Experimental

3.1. Materials

C₆F₅H (>98%), C₆F₅Cl (>98%) and ClC₆F₄H (>98%) were purchased from J&K. DMSO-*d*₆ (>99.8 of deuterium) was from Cambridge Isotopes Laboratories (CIL). DMSO (>99.5%) was purchased from Beijing Chemical Plant (Beijing, China).

3.2. FTIR Spectroscopy

FTIR spectra over the range from 4000 to 650 cm⁻¹ were collected at room

temperature ($\sim 25^\circ\text{C}$) using a Nicolet 5700 FTIR spectrometer, equipped with a DTGS detector. The attenuated total reflection (ATR) cells, made of trapezoidal ZnSe and Ge crystals with incident angles of 45° and 60° corresponding to 12 and 7 reflections, respectively, were employed. The Ge crystal, with fewer numbers of reflections and thus shorter effective light path, was used to examine the strong stretching bands of C–Cl and S=O. The ZnSe crystal was used to examine the stretching bands of C–H and C–D. All spectra were recorded with a resolution of 2 cm^{-1} , 16 parallel scans, and a zero filling factor of 2. For each sample, three parallel measurements were carried out. The refractive indexes of solutions were measured with an Abbe refractometer at 25°C . The formula suggested by Hansen⁵⁰ was used to do the ATR corrections.

3.3. Excess Infrared Spectroscopy

The theory of excess infrared spectroscopy has been described in detail elsewhere.^{30,31} Briefly, an excess infrared spectrum is defined as the difference between the spectrum of a real solution and that of the respective ideal solution under identical conditions. The working equation in calculating the excess infrared spectrum is

$$\varepsilon^{\text{E}} = \frac{A}{d(C_1 + C_2)} - (x_1\varepsilon_1^* + x_2\varepsilon_2^*) \quad (1)$$

where A is the absorbance of the mixture, d is the light path length, C_i , x_i and ε_i^* are the molarity, mole fraction and molar absorption coefficient of component i in its pure state, respectively. If our attention is the overall absorbance of a particular absorption band, the excess molar absorbance of the band can be expressed by its integrated value.

Matlab 7.0 (Math Works Inc., Natick, MA) was used to manipulate spectral data pretreatment, i.e., the subtraction, truncation and baseline correction, to calculate excess infrared spectra and to do the integration of the bands in the excess infrared spectra.

3.4. Two-Dimensional Correlation Spectroscopy

Standard 2D correlation spectral analysis was performed using Matlab 7.0, based on the algorithm developed by Noda.⁴⁰ In order to remove the linear contribution to absorbance by concentration variation and thus to obtain the information of specific interactions, the selected bands were normalized with the modified component-normalization method, namely the absorption bands of $\nu(\text{C-H})$ and $\nu(\text{C-Cl})$ in excess infrared spectra were divided by the corresponding molarity of $\text{ClC}_6\text{F}_4\text{H}$.^{33,51} The average of all the spectra over the full concentration range was used as the reference spectrum. In the 2D correlation contour map, solid (red) and dashed (blue) lines represent positive and negative correlation intensities, respectively.

3.5. NMR Measurements

The ^1H NMR and ^{19}F NMR measurements were carried out on JEOL JNM-ECA 300 NMR (300 MHz) and 600 NMR (600 MHz) spectrometers at 298 K, respectively. TMS dissolved in CCl_4 and pure CF_3COOH were used as external standards for ^1H NMR and ^{19}F NMR, respectively, to avoid their influence on the chemicals in the binary mixtures.

3.6. Quantum Chemical Calculations

All computations were performed with the Gaussian 03 program.⁵² We used the

second-order many-body perturbation theory (MP2) with the aug-cc-pVDZ basis set to optimize electrostatic surface potential, molecular energy, geometry, vibrational frequency, vibrational intensity and the natural population analysis (NPA) charge of both the four isolated single molecules C_6F_5H , C_6F_5Cl , ClC_6F_4H , DMSO, and their complexes. The optimized geometries at local energy minimum were ensured by the absence of imaginary vibrational frequency. The interaction energy was estimated as the difference between the total energy of the complex and the sum of total energies of the two monomers. Meanwhile, the basis set superposition error (BSSE) correction computed via the counterpoise method of Boys and Bernardi was estimated to obtain accurate interaction energies of the complexes.⁵³ The NPA charges were obtained using the nature bond orbital (NBO) approach.⁵⁴ To evaluate the distance dependence of the halogen-bond energy and hydrogen-bond energy, single point energies were calculated by changing the distance between an electron donor (oxygen atom in DMSO) and an electron acceptor (chlorine atom in C_6F_5Cl and hydrogen atom in C_6F_5H). The electrostatic surface potential $V(r)$ at any point r in the surrounding space is given by

$$V(r) = \sum_A \frac{Z_A}{|R_A - r|} - \int \frac{\rho(r') dr'}{|r' - r|} \quad (2)$$

where Z_A is the charge in nucleus A, located at R_A , and $\rho(r)$ is the electronic density.^{14,15}

4. Conclusions

By taking three chlorine- and/or hydrogen-containing fluoro-benzene derivatives as model donor molecules and DMSO as an acceptor, we performed a comparative study

on halogen-bonds and hydrogen-bonds. Several conclusions can be drawn. (1) Like hydrogen-bonds, halogen-bonds are directional. The latter are stricter in this regard, only slightly deviated from 180° . (2) Upon complexation, the C–H and C–Cl groups in C_6F_5H and ClC_6F_4H are all elongated concomitant with decreases in the corresponding stretching frequencies (red-shift) and increase in infrared intensities. (3) The interaction energy of the chlorine halogen-bond is much weaker than that of the hydrogen-bond. Thus, for ClC_6F_4H , DMSO prefers to interact with the C–H rather than the C–Cl as evidenced by 2D-COS, quantum chemical calculation and ^{19}F NMR. The interaction energies were found to depend on the bond length in the forms of $1/r^{3.3}$ and $1/r^{3.1}$ for hydrogen-bond and halogen-bond, respectively. Thus the interaction energy of the halogen-bond decays more slowly than that of the hydrogen-bond. To the best of our knowledge, this is the first report on the bond-length dependence of the interaction potential energy of a halogen-bond. (4) Upon the formation of hydrogen/halogen-bonds, electron transfers from DMSO to C_6F_5H , C_6F_4ClH and C_6F_5Cl . Although the methyl groups of DMSO do not participate directly into the formation of the halogen/hydrogen-bond, they donate electrons to the S=O group and contribute positively to the stability of the complexes. The “back groups”, therefore, are not inert. (5) Other than providing experimental evidences on the formation of halogen/hydrogen-bonds in the three systems, the FTIR band of $\nu(C-Cl)$ in the C_6F_5Cl -DMSO mixtures show an isobestic point. This strongly suggests the presence of two dominate forms of the interactive partners, with and without the halogen-bond. In the other two systems containing either C_6F_5H or

$\text{ClC}_6\text{F}_4\text{H}$, although no isobestic point was observed, distinct new peaks in the lower wavenumber region were seen (Figure 5) concerning the $\nu(\text{aromatic C-H})$. This means that stable complexes were also formed in these two systems. These compared studies on the interactions between three fluoro-benzene derivatives and DMSO provide in-depth information for understanding the halogen-bond and hydrogen-bond interactions in solution.

Acknowledgements

This work was partially supported by the Natural Science Foundation of China (Grant Nos. 21133009, 21273130) and a national “863” program (No. 2012AA030306).

References and Notes

- (1) L. Brammer, E. A. Bruton and P. Sherwood, *Cryst. Growth Des.*, 2001, **1**, 277–290.
- (2) T. Steiner, *Angew. Chem., Int. Ed.*, 2002, **41**, 48–76.
- (3) G. R. Desiraju and T. Steiner, *The Weak Hydrogen Bond*, Oxford University Press, Oxford, 1999.
- (4) S. Scheiner, *Hydrogen Bonding*, Oxford University Press, New York, 1997.
- (5) K. Rissanen, *CrystEngComm*, 2008, **10**, 1107–1113.
- (6) T. Takeuchi, Y. Minato, M. Takase and H. Shinmori, *Tetrahedron Lett.*, 2005, **46**, 9025–9027.
- (7) P. Metrangolo, F. Meyer, T. Pilati, G. Resnati and G. Terraneo, *Angew. Chem., Int. Ed.*, 2008, **47**, 6114–6127.
- (8) P. Auffinger, F. A. Hays, E. Westhof and P. S. Ho, *Proc. Natl. Acad. Sci. U. S. A.*, 2004, **101**, 16789–16794.
- (9) Y. X. Lu, Y. Wang and W. L. Zhu, *Phys. Chem. Chem. Phys.*, 2010, **12**, 4543–4551.
- (10) R. H. Crabtree, P. E. M. Siegbahn, O. Eisenstein, A. L. Rheingold and T. F. Koetzle, *Acc. Chem. Res.*, 1996, **29**, 348–354.
- (11) F. Guthrie, *J. Chem. Soc.*, 1863, **16**, 239–244.
- (12) A. C. Legon, *Phys. Chem. Chem. Phys.*, 2010, **12**, 7736–7747.
- (13) P. Metrangolo, J. S. Murray, T. Pilati, P. Politzer, G. Resnati and G. Terraneo, *CrystEngComm*, 2011, **13**, 6593–6596.
- (14) P. Politzer and J. S. Murray, *ChemPhysChem*, 2013, **14**, 278–294.
- (15) P. Politzer, J. S. Murray and T. Clark, *Phys. Chem. Chem. Phys.*, 2010, **12**, 7748–7757.
- (16) T. Clark, M. Hennemann, J. S. Murray and P. Politzer, *J. Mol. Model.*, 2007, **13**, 291–296.
- (17) P. Politzer and J. S. Murray, T. Clark, *Phys. Chem. Chem. Phys.*, 2013, **15**, 11178–11189.

- (18) K. E. Riley, J. S. Murray, J. Fanfrlík, J. Řezáč, R. J. Solá, M. C. Concha, F. M. Ramos and P. Politzer, *J. Mol. Model.*, 2011, **17**, 3309–3318.
- (19) P. Metrangolo, H. Neukirch, T. Pilati and G. Resnati, *Acc. Chem. Res.*, 2005, **38**, 386–395.
- (20) W. Z. Wang, N. B. Wong, W. X. Zheng and A. M. Tian, *J. Phys. Chem. A*, 2004, **108**, 1799–1805.
- (21) Q. Z. Li, H. F. Yuan, B. Jing, Z. B. Liu, W. Z. Li, J. B. Cheng, B. A. Gong and J. Z. Sun, *Mol. Phys.*, 2010, **108**, 611–617.
- (22) J. P. M. Lommerse, A. J. Stone, R. Taylor and F. H. Allen, *J. Am. Chem. Soc.*, 1996, **118**, 3108–3116.
- (23) H. Umeyama and K. Morokuma, *J. Am. Chem. Soc.*, 1977, **99**, 1316–1332.
- (24) M. G. Sarwar, B. Dragisic, L. J. Salsberg, C. Gouliaras and M. S. Taylor, *J. Am. Chem. Soc.*, 2010, **132**, 1646–1653.
- (25) T. Beweries, L. Brammer, N. A. Jasim, J. E. McGrady, R. N. Perutz and A. C. Whitwood, *J. Am. Chem. Soc.*, 2011, **133**, 14338–14348.
- (26) Z. W. Yu and P. J. Quinn, *Biosci. Rep.*, 1994, **14**, 259–281.
- (27) T. Clark, J. S. Murray, P. Lane and P. Politzer, *J. Mol. Model.*, 2008, **14**, 689–697.
- (28) X. Y. Ma, K. C. Cai and J. P. Wang, *J. Phys. Chem. B*, 2011, **115**, 1175–1187.
- (29) Q. J. Shen and W. J. Jin, *Phys. Chem. Chem. Phys.*, 2011, **13**, 13721–13729.
- (30) Q. Z. Li, G. S. Wu and Z. W. Yu, *J. Am. Chem. Soc.*, 2006, **128**, 1438–1439.
- (31) Q. Z. Li, N. N. Wang, Q. Zhou, S. Q. Sun and Z. W. Yu, *Appl. Spectrosc.*, 2008, **62**, 166–170.
- (32) Y. Koga, F. Sebe, T. Minami, K. Otake, K. Saitow and K. Nishikawa, *J. Phys. Chem. B*, 2009, **113**, 11928–11935.
- (33) N. N. Wang, Q. Jia, Q. Z. Li and Z. W. Yu, *J. Mol. Struct.*, 2008, **883–884**, 55–60.
- (34) N. N. Wang, Q. Z. Li and Z. W. Yu, *Appl. Spectrosc.*, 2009, **63**, 1356–1362.
- (35) Q. G. Zhang, N. N. Wang and Z. W. Yu, *J. Phys. Chem. B*, 2010, **114**, 4747–4754.
- (36) N. N. Wang, Q. G. Zhang, F. G. Wu, Q. Z. Li and Z. W. Yu, *J. Phys. Chem. B*, 2010, **114**, 8689–8700.

- (37) Q. G. Zhang, N. N. Wang, S. L. Wang and Z. W. Yu, *J. Phys. Chem. B*, 2011, **115**, 11127–11136.
- (38) Y. Z. Zheng, N. N. Wang, J. J. Luo, Y. Zhou and Z. W. Yu, *Phys. Chem. Chem. Phys.*, 2013, **15**, 18055–18064.
- (39) N. N. Wang, Y. Wang, H. F. Cheng, Z. Tao, J. Wang and W. Z. Wu. *RSC Adv.*, 2013, **3**, 20237–20245.
- (40) I. Noda, *Appl. Spectrosc.*, 1993, **47**, 1329–1336.
- (41) I. Noda and Y. Ozaki, *Two-Dimensional Correlation Spectroscopy: Applications in Vibrational and Optical Spectroscopy*, Wiley, Chichester, 2004, pp. 22–23.
- (42) S. G. Frankiss and D. J. Harrison, *Spectrochim. Acta*, 1975, **31A**, 1839–1864.
- (43) W. D. Horrocks Jr and F. A. Cotton, *Spectrochim. Acta*, 1961, **17**, 134–147.
- (44) J. R. Murdoch and A. J. Streitwieser, *J. Phys. Chem.*, 1981, **85**, 3352–3354.
- (45) L. Pauling, *The Nature of the Chemical Bond*, Cornell University Press, New York, 3rd ed., 1960.
- (46) Z. P. Shields, J. S. Murray and P. Politzer, *Int. J. Quantum Chem.*, 2010, **110**, 2823–2832.
- (47) K. Wendler, J. Thar, S. Zahn and B. Kirchner, *J. Phys. Chem. A*, 2010, **114**, 9529–9536.
- (48) D. Hauchecorne, B. J. van der Veken, W. A. Herrebout and P. E. Hansen, *Chem. Phys.*, 2011, **381**, 5–10.
- (49) P. Metrangolo, W. Panzeri, F. Recupero and G. Resnati, *J. Fluorine Chem.*, 2002, **114** 27–33.
- (50) W. N. Hansen, *Spectrochim. Acta*, 1965, **21**, 815–833.
- (51) Z. W. Yu, L. Chen, S. Q. Sun and I. Noda, *J. Phys. Chem. A*, 2002, **106**, 6683–6687.
- (52) M. J. Frisch, G. W. Trucks, H. B. Schlegel, G. E. Scuseria, M. A. Robb, J. R. Cheesman, V. G. Zakrzewski, J. A., Jr. Montgomery, R. E. Stratmann, J. C. Burant, S. Dapprich, J. M. Millam, A. D. Daniels, K. N. Kudin, M. C. Strain, O. Farkas, J. Tomasi, V. Barone, M. Cossi, R. Cammi, B. Mennucci, C. Pomelli, C. Adamo, S. Clifford, J. Ochterski, A. Petersson, P. Y. G. Ayala, Q. Cui, K.

Morokuma, D. K. Malick, A. D. Rabuck, K. Raghavachari, J. B. Foresman, J. Cioslowski, J. V. Ortiz, A. G. Baboul, B. B. Stefanov, G. Liu, A. Liashenko, P. Piskorz, I. Komaromi, R. Gomperts, R. L. Martin, D. J. Fox, T. Keith, M. A. Al-Laham, C. Y. Peng, A. Nanayakkara, C. Gonzalez, M. Challacombe, P. M. W. Gill, B. Johnson, W. Chen, M. W. Wong, J. L. Andres, C. Gonzalez, M. Head-Gordon, E. S. Replogle, J. A. Pople, *Gaussian 03, Revision B. 03*, Gaussian Inc., Pittsburgh, PA, 2003.

(53) S. F. Boys and F. Bernardi, *Mol. Phys.*, 1970, **19**, 553–566.

(54) A. E. Reed, L. A. Curtiss and F. Weinhold, *Chem. Rev.*, 1988, **88**, 899–926.

Table 1. Selected bond length (Å) of the optimized complexes. The C–H represent aromatic C–H. The data in the parentheses represent the changes in bond length upon complex.

Complex	r(C–H)	r(C–Cl)
C ₆ F ₅ H–DMSO	1.091 (0.007)	
C ₆ F ₅ Cl–DMSO		1.711 (0.002)
ClC ₆ F ₄ H–DMSO	1.090 (0.007)	1.715 (0.002)

Table 2. Selected vibrational frequency (ν/cm^{-1}) and infrared intensity ($I/\text{km mol}^{-1}$) of the optimized complexes. The C–H represent aromatic C–H. The data in the parentheses represent the vibrational frequency and intensity changes upon complexation.

Complex	$\nu(\text{C-H})$	$I(\text{C-H})$	$\nu(\text{C-Cl})$	$I(\text{C-Cl})$
C ₆ F ₅ H–DMSO	3157.67	318.13		
	(–98.47)	(310.93)		
C ₆ F ₅ Cl–DMSO			887.43	151.14
			(–0.14)	(4.74)
ClC ₆ F ₄ H–DMSO	3165.93	351.99	915.44	101.17
	(–89.17)	(344.58)	(–3.00)	(14.18)

Table 3. Charges (q in e) on selected atoms and groups and charge change (CC) of the entire DMSO molecule. The data in the parentheses represent the charge changes of the corresponding atoms or groups upon complexation. H represents the hydrogen atoms in C_6F_5H and ClC_6F_4H . Negative values mean increases in charge density.

Complex	H	methyl	Cl	O	CC
C_6F_5H -DMSO	0.288 (0.046)	-0.202 (0.035)		-0.979 (-0.025)	0.018
C_6F_5Cl -DMSO		-0.215 (0.022)	0.133 (0.034)	-0.966 (-0.012)	0.009
ClC_6F_4H -DMSO	0.287 (0.045)	-0.205 (0.032)	0.087 (-0.009)	-0.979 (-0.025)	0.014

Table 4. Charge changes on fluorine atoms upon complexation between three benzene derivatives and DMSO. The H and Cl atoms in bold face are the ones forming hydrogen/halogen-bonds. Negative values mean increases in charge density.

Complex	1	2	3
C ₆ F ₅ H -DMSO	-0.004	-0.017	-0.009
C ₆ F ₅ Cl -DMSO	-0.004	-0.008	-0.007
ClC ₆ F ₄ H -DMSO	-0.016	-0.008	
HC ₆ F ₄ Cl -DMSO	-0.006	-0.008	
DMSO-ClC ₆ F ₄ H -DMSO	-0.020	-0.018	

Figure Captions

Figure 1. The computed electrostatic surface potentials of fluoro-benzene derivatives and DMSO.

Figure 2. Partial IR spectra of pure C_6F_5H , ClC_6F_4H , C_6F_5Cl , DMSO, and $DMSO-d_6$ in selected wavelength regions.

Figure 3. Synchronous and asynchronous 2D-COS contour maps of $\nu(C-H)$ and $\nu(C-Cl)$ of ClC_6F_4H in the dilution process. The dashed (blue) lines represent negative correlation intensities. Positive values are absent in the selected wavelength region.

Figure 4. ATR-FTIR (A) and excess infrared spectra (B) of $C_6F_5Cl-DMSO-d_6$ system in the range of $\nu(C-Cl)$. From top to bottom, the mole fraction of $DMSO-d_6$ increases from 0 to 1 in A with an increment of about 0.1. The dashed and dash-dotted lines depict spectra of pure C_6F_5Cl and $DMSO-d_6$ in (A). (C) is the normalized IR spectra by the corresponding molarity of C_6F_5Cl and the light path, and dashed line depicts spectrum of pure C_6F_5Cl .

Figure 5. ATR-FTIR (upper) and excess infrared (lower) spectra of $C_6F_5H-DMSO-d_6$ (A, C) and $ClC_6F_4H-DMSO-d_6$ (B, D) systems in the region of aromatic C-H stretching vibration regions. From top to bottom, the mole fraction of $DMSO-d_6$ increases from 0 to 1 in A and B with an increment of about 0.1. The dashed and dash-dotted lines depict spectra of pure C_6F_5H , ClC_6F_4H and $DMSO-d_6$.

Figure 6. ATR-FTIR (upper) and excess infrared (lower) spectra of C_6F_5H -DMSO- d_6 (A, D), ClC_6F_4H -DMSO- d_6 (B, E) and C_6F_5Cl -DMSO- d_6 (C, F) systems in the range of $\nu_s(C-D)$. From top to bottom, the mole fraction of DMSO- d_6 decreases from 1 to 0 in A, B and C with a decrement of about 0.1. The dashed and dash-dotted lines depict spectra of pure C_6F_5H , C_6F_5Cl , C_6F_4ClH and DMSO- d_6 .

Figure 7. Optimized geometries and corresponding interaction energies of C_6F_5H -DMSO, ClC_6F_4H -DMSO and C_6F_5Cl -DMSO complexes. Hydrogen-bonds and halogen-bonds are denoted by dashed lines, and the corresponding hydrogen-bond and halogen-bond distances (Å, dark red) and angles ($^\circ$, blue) are labeled.

Figure 8. Interaction energies of halogen-bond complex C_6F_5Cl -DMSO and hydrogen-bond complex C_6F_5H -DMSO as functions of Cl-O and H-O distance.

Figure 9. 1H NMR assignments of pure C_6F_5H , ClC_6F_4H and DMSO (A) and chemical shift changes of the hydrogen atoms in the benzene derivatives (B) and in the methyl groups of DMSO (C) in C_6F_5H -DMSO, ClC_6F_4H -DMSO and C_6F_5Cl -DMSO systems.

Figure 10. ^{19}F NMR assignments of pure C_6F_5H , ClC_6F_4H and C_6F_5Cl (A) and chemical shift changes of the fluorine atoms in the three molecules upon interacting with DMSO.

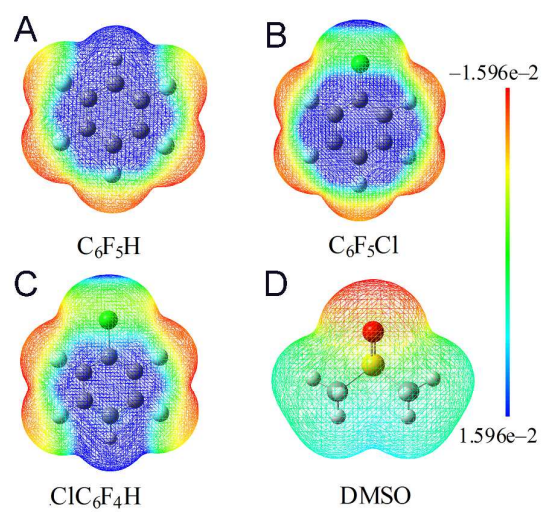


Figure 1

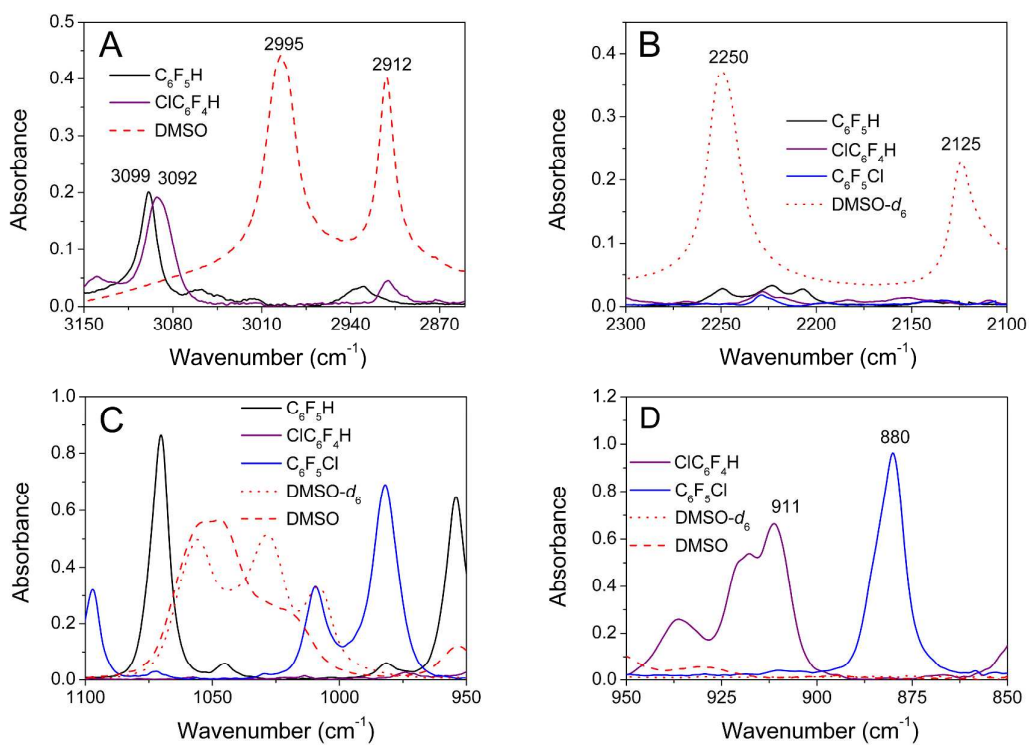
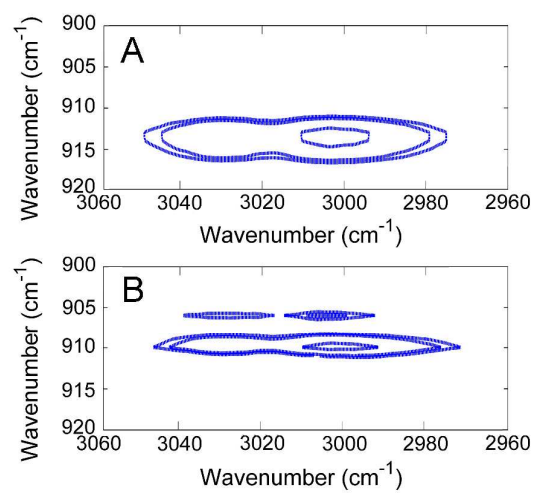


Figure 2

**Figure 3**

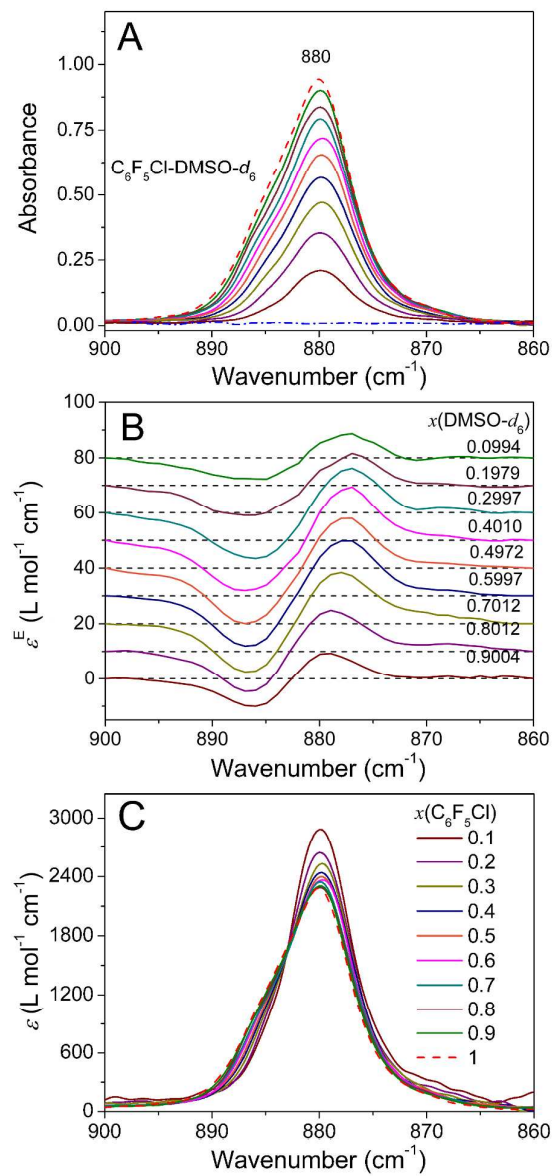


Figure 4

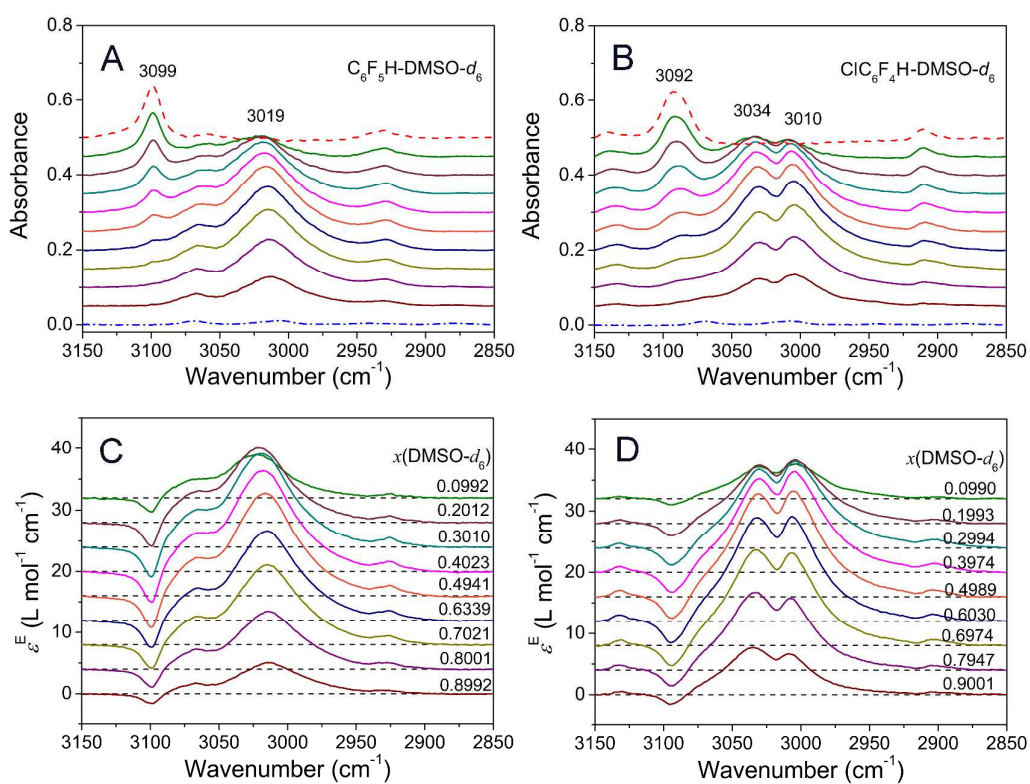


Figure 5

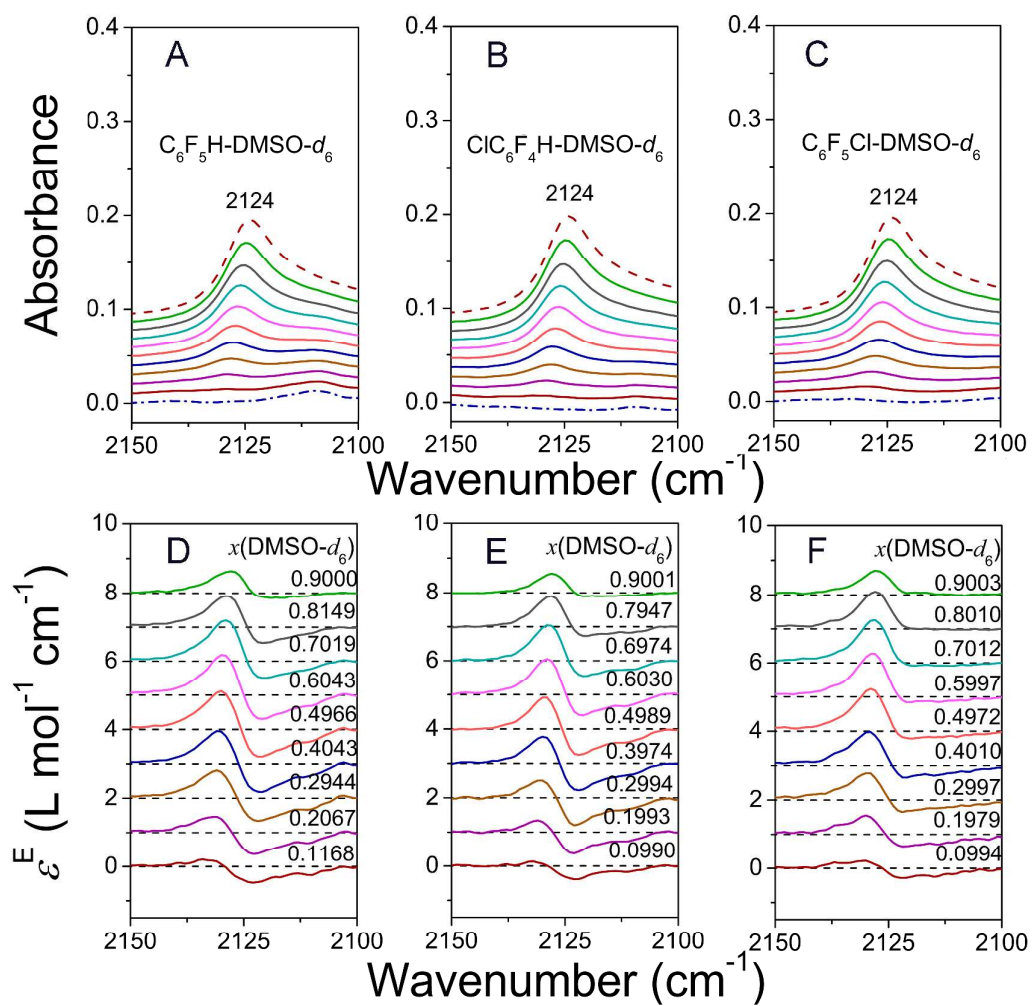


Figure 6

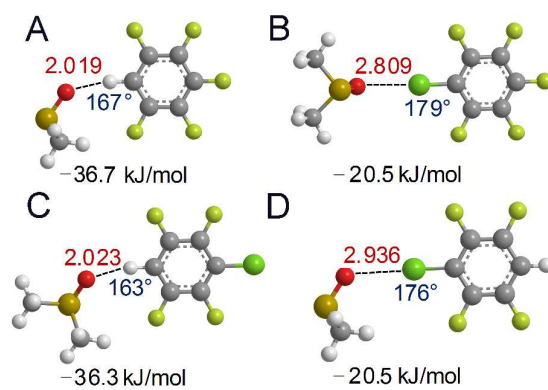


Figure 7

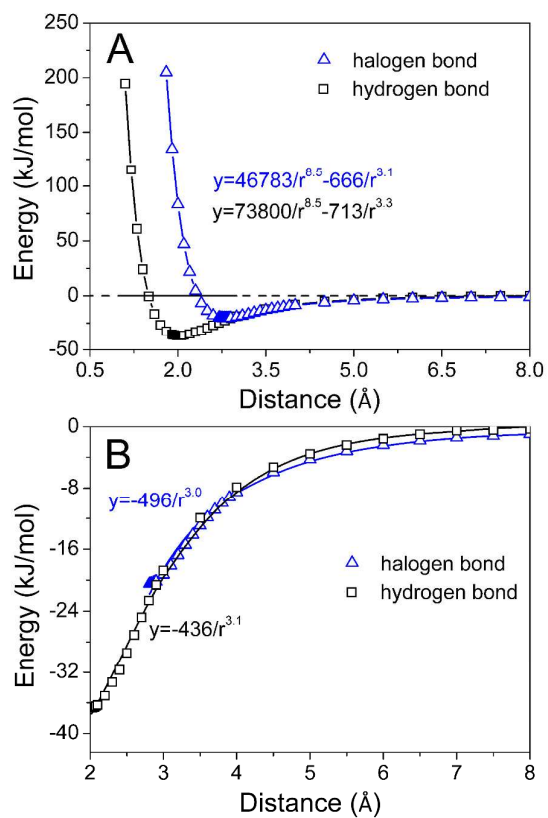


Figure 8

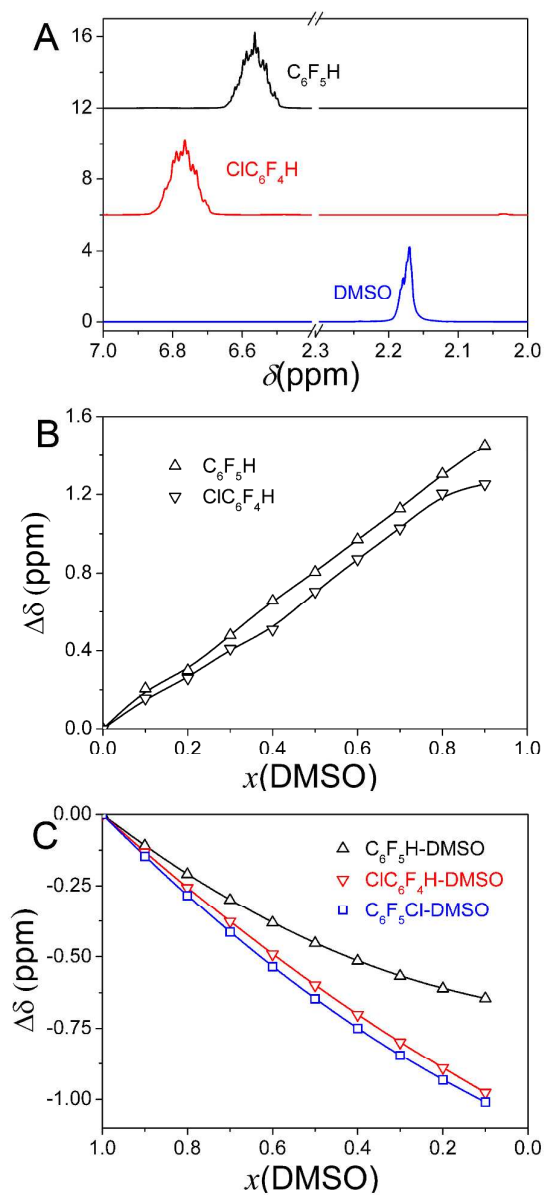


Figure 9

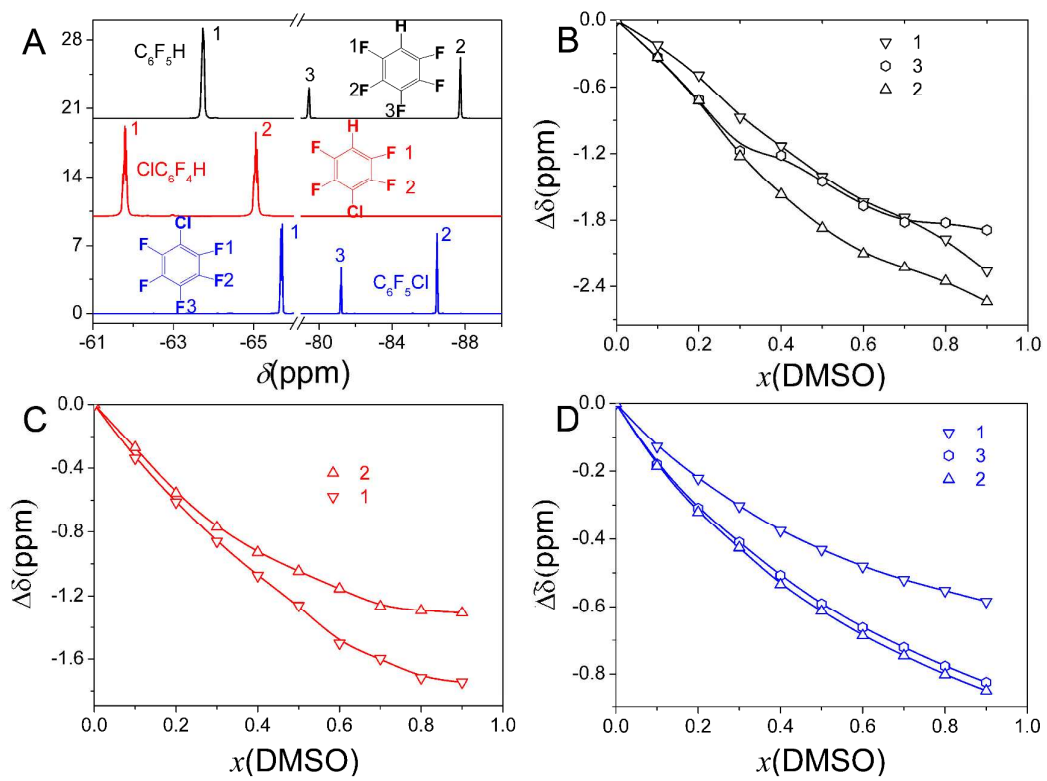
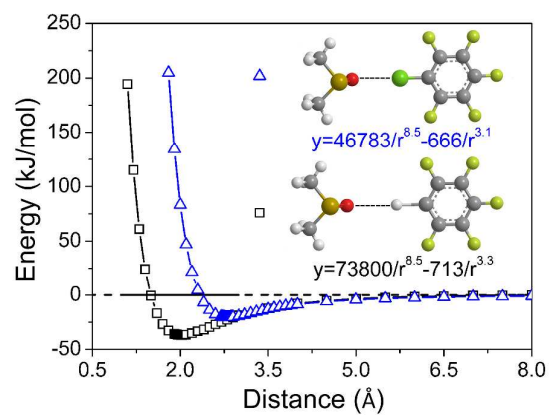


Figure 10



TOC. Interaction energies of halogen-bond C₆F₅Cl-DMSO and hydrogen-bond complex C₆F₅H-DMSO as functions of Cl-O and H-O distance